NIH Public Access
Author Manuscript
Mol Microbiol. Author manuscript; available in PMC 2011 August 1.

Published in final edited form as:
Mol Microbiol. 2010 August ; 77(3): 605–617. doi:10.1111/j.1365-2958.2010.07232.x.

M. tuberculosis intramembrane protease Rip1 controls transcription through three anti-sigma factor substrates

Joseph G. Sklar[a,e], **Hideki Makinoshima**[d,e], **Jessica Schneider**[c], and **Michael S. Glickman**[a,b,c,*]

[a] Immunology Program, Sloan-Kettering Institute

[b] Division of Infectious Diseases, Memorial Sloan-Kettering Cancer Center, New York, New York 10021, USA

[c] Program in Immunology and Microbial Pathogenesis, Weil Cornell Graduate School of Biomedical Sciences

Summary

Regulated intramembrane proteolysis (RIP) is a mechanism of transmembrane signal transduction that functions through intramembrane proteolysis of substrates. We previously reported that the RIP metalloprotease Rv2869c (Rip1) is a determinant of *Mycobacterium tuberculosis* (Mtb) cell envelope composition and virulence, but the substrates of Rip1 were undefined. Here we show that Rip1 cleaves three transmembrane anti-Sigma factors: anti-SigK, anti-SigL, and anti-SigM, negative regulators of Sigma K, L, and M. We show that transcriptional activation of *katG* in response to phenanthroline requires activation of SigK and SigL by Rip1 cleavage of anti-SigK and anti-SigL. We also demonstrate a Rip1 dependent pathway that activates the genes for the mycolic acid biosynthetic enzyme KasA and the resuscitation promoting factor gene RpfC, but represses the bacterioferritin encoding gene *bfrB*. Regulation of these three genes by Rip1 is not reproduced by deletion of Sigma K, L, or M, either indicating a requirement for multiple Rip1 substrates or additional arms of the Rip1 pathway. These results identify a branched proteolytic signal transduction system in which a single intramembrane protease cleaves three anti-sigma factor substrates to control multiple downstream pathways involved in lipid biosynthesis and defense against oxidative stress.

Keywords

Intramembrane proteolysis; *M. tuberculosis*; sigma factor; signal transduction; anti-sigma factors

Introduction

Mycobacterium tuberculosis infection is an ongoing global health crisis that has not abated with present control measures (Dye, 2006). Despite the availability of effective antimicrobials that cure drug sensitive *M. tuberculosis* infection, these regimens are prolonged compared to antibiotic therapy of more acute respiratory infections (Council, 1984). The prolonged therapy of *M. tuberculosis* infection is difficult to administer in resource poor settings and non-compliance with drug regimens breeds antibiotic resistance

[*]Correspondence should be addressed to Glickman MS., Box 9, Division of Infectious Diseases, Memorial Sloan-Kettering, Cancer Center, New York, New York 10021, USA, Phone: +1-1-646-888-2368, glickmam@mskcc.org.
[d]Present address Ohoku University Graduate School of Medicine 2-1, Seiryo-machi, Aoba-ku Sendai 980-8575Miyagi, Japan
[e]equal contribution

NIH-PA Author Manuscript
NIH-PA Author Manuscript
NIH-PA Author Manuscript

NIH-PA Author Manuscript

NIH-PA Author Manuscript

NIH-PA Author Manuscript

(Dye *et al.*, 2002) and treatment failure. For these reasons, new antibiotics that might shorten therapy are badly needed.

To survive in its host, *M. tuberculosis* must respond to a variety of host inflicted stresses, including iron limitation, reactive nitrogen and oxygen intermediates, and starvation (De Voss *et al.*, 2000, Schnappinger *et al.*, 2003, Stallings *et al.*, 2009). These stresses require dedicated signal transduction systems that transmit information inside the cell, allowing for the modulation of gene expression programs. In bacteria, one such widely distributed mechanism of signal transduction controls the availability of extracytoplasmic function (ECF) sigma factors, alternative sigma factors that direct RNA polymerase to specific promoters. ECF sigma factors are often held inactive by transmembrane anti-sigma factors, which are degraded by proteolysis in response to extracellular stimuli. Cleavage of the anti-sigma factor by a site-one protease (S1P) initiates signaling and is immediately followed by site-two cleavage by the site two protease (S2P), which releases the sigma factor from the membrane, thereby activating the pathway (Urban, 2009). Well studied prokaryotic S1P/S2P/anti-sigma factor/sigma factor systems include *Escherichia coli* DegS/RseP/RseA/SigE, which responds to unfolded outer membrane proteins (Alba *et al.*, 2002, Kanehara *et al.*, 2002), and *Bacillus subtilis* PrsW/RasP/RsiW/SigW, which responds to alkaline shock and antimicrobial peptides (Ellermeier & Losick, 2006, Heinrich & Wiegert, 2006). Recent evidence from *B. subtilis* suggests that additional proteases participate in trimming the antisigma factor before site-two cleavage, adding additional complexity to these signal transduction systems (Heinrich *et al.*, 2009).

We previously identified Rip1 as a major virulence determinant of *M. tuberculosis* through its role in regulating cell envelope composition (Makinoshima & Glickman, 2005). Rip1 is a member of the S2P class of proteases, which are widely prevalent in bacterial genomes (Makinoshima & Glickman, 2006, Kinch *et al.*, 2006). However, the molecular mechanisms by which Rip1 controls downstream gene expression are not defined. In this study, we demonstrate that Rip1 participates in signaling across the cell envelope through proteolysis of three anti-sigma factor substrates.

Results

Bioinformatic Identification of 4 *M. tuberculosis* anti-sigma factors as candidate substrates for Rip1

Based on S2P pathways in other bacteria, we hypothesized that potential substrates of Rip1 would be transmembrane anti-sigma factors. In four of the 13 *M. tuberculosis* sigma factor operons (*sigD*, *sigK*, *sigL* and *sigM*), known or putative anti-sigma factor encoding genes are located immediately downstream of the genes for their associated ECF sigma factors. Anti-SigK (RskA, Rv0444c) and anti-SigL (RslA, Rv0736) were previously shown to bind their cognate sigma factor (Said-Salim *et al.*, 2006, Dainese *et al.*, 2006, Hahn *et al.*, 2005), but Rv3912 (RsmA) and Rv3413c (RsdA) have not been previously examined. Hydropathy profiling of these four proteins revealed a single central predicted transmembrane domain with a similarly sized C terminal domain in anti-SigK, L, and M, but an extended C terminus in anti-SigD (Figure 1). Furthermore, the RskA, RslA, and RsmA proteins were recently predicted to contain a conserved structural module present in diverse anti-sigma factors (Campbell *et al.*, 2007). Based on these findings, we considered that these proteins were possible substrates for the three S2P family RIP proteases of *M. tuberculosis*.

Rip1, but not Rip2 or Rip3, cleaves three anti-sigma factors in *M. tuberculosis*

To test whether these anti-sigma factors are substrates of S2P family RIP proteases in *M. tuberculosis*, we constructed anti-sigma factors with N-terminal Hemagglutinin (HA) tags

NIH-PA Author Manuscript

NIH-PA Author Manuscript

NIH-PA Author Manuscript

and examined the steady-state levels of these proteins in wild type *M. tuberculosis* and cells lacking Rip1. In wild type cells, RsdA, RskA, RslA, and RsmA were detected at their predicted unprocessed molecular sizes (Figure 2A-D, WT lanes). In contrast, in cells lacking Rip1, we observed the accumulation of smaller products of RskA, RslA, and RsmA of approximately 15–20 kD (Figure 2B-D, ΔM lanes) in addition to full-length protein. No RsdA intermediates were detected in cells lacking Rip1 (Figure 2A). Because the HA tag is at the N terminus of each protein, the smaller products observed in the *rip1* null strain must be the result of C terminal truncation. The size of the accumulated intermediates suggests that the C terminal truncation occurred on the extracytoplasmic side of the transmembrane domain (see schematic in figure 2E showing full length and predicted ΔC anti-sigma factors). The accumulation of truncated anti-sigma factors in the *rip1* mutant, but not wild type, suggests that this intermediate is rapidly processed by Rip1 in wild type cells and is therefore observed at steady state only in cells lacking *rip1*. The pattern of anti-sigma factor intermediates observed in the Δ*rip1* strain is similar to the RsiW fragment that accumulates in the *rasP* null mutant of *B. subtilis* after PrsW cleavage (Ellermeier & Losick, 2006, Schobel *et al.*, 2004) and the RseA fragment after DegS cleavage in the absence of RseP (Alba et al., 2002, Kanehara et al., 2002).

The truncated anti-sigma factors observed in the *rip1* mutant coexist with a substantial amount of full-length protein, indicating that cleavage by the S1P is incomplete under these assay conditions. This finding may indicate that the activation signals for these sigma factor regulons are not present under the conditions tested, as was observed in the SigK, SigL and SigM pathways (Agarwal *et al.*, 2006, Dainese et al., 2006, Hahn et al., 2005, Raman *et al.*, 2006, Said-Salim et al., 2006). To more clearly interrogate the role of Rip1 in anti-sigma factor cleavage, we expressed C terminally truncated versions of RsdA, RskA, RslA, and RsmA in wild type and Δ*rip1* cells, reasoning that these truncated proteins would not require site one cleavage to be substrates of Rip1 (Schobel et al., 2004). RsmA-154 and RskA-160 accumulated in Δ*rip1* cells but not in wild type cells (Figure 2F). We could not examine a truncated RslA as we were unable to transform Δ*rip1* cells with the truncated RslA construct. RsdA-192 did not accumulate in wild type or Δ*rip1* cells (Figure 2F), suggesting that it can be degraded by a S2P other than Rip1. Taken together, we interpret these results to indicate that second site cleavage of RskA, RslA, and RsmA requires the Rip1 protease.

The *M. tuberculosis* chromosome encodes two other predicted S2Ps, *rv0359* (*rip2)* and *rv2625c* (*rip3).* To examine whether these proteases are involved in processing anti-sigma D,K,L,M, we examined our HA tagged anti-sigma factor proteins in cells lacking these proteases. In *M. tuberculosis*Δ*rip2* and Δ*rip3*, all three anti-sigma factors remained unprocessed as in wild type cells and no proteolytic intermediates were detected (Figure S1, A-B). Therefore, under our assay conditions, we conclude that neither Rip2 nor Rip3 are required for processing these four anti-sigma factors.

Rip1 mediated cleavage of anti-sigma factors is conserved in *M. smegmatis*

To further examine the molecular requirements for anti-sigma factor processing by Rip1, we reconstituted the processing event in the fast growing mycobacterium *M. smegmatis*. The *M. smegmatis* chromosome encodes two S2P family members, one an apparent ortholog of Rip1 (MSmeg_2579, MSm*rip1*, 68% identity) and one of Rip2 (MSmeg_0756, MSm*rip2*, 68% identity). We deleted each of these genes from the *M. smegmatis* chromosome by two-step allelic exchange, leaving unmarked deletion mutations (data not shown). We then examined the HA tagged *M. tuberculosis* anti-sigma factors in each of these *M. smegmatis* protease mutants. We observed full length RsdA, RskA, RslA, and RsmA in the MSm*rip2* mutant and no proteolytic intermediates were observed (data not shown). In contrast, in the MSm*rip1* null strain, we observed C terminally truncated intermediates of RskA, RslA, and RsmA (figure 3A). These results indicated that Rip1 and MSmRip1 are functionally

NIH-PA Author Manuscript

NIH-PA Author Manuscript

NIH-PA Author Manuscript

conserved with respect to anti-sigma factor cleavage. We then expressed truncated anti-sigma factors in the MSm*rip1* null strain and observed accumulation of all truncated anti-sigma factors except for RsdA (figure 3B)

To show that the accumulation of anti-sigma factor intermediates was the result of loss of Rip1 proteolytic activity, we complemented the MSm*rip1* mutant with *M. tuberculosis* Rip1 and Rip1-H21A, encoding a Rip1 protein with an inactivating mutation in the protease active site. Complementation with *rip1* abolished accumulation of RskA160 (figure 3C) and RslA161 (figure 3D), whereas complementation with the H21A active site mutant resulted in accumulation of both RskA160 and RslA161 similar to the mutant strain (Figure 3C-D). These experiments strongly indicate that RskA, RslA, and RsmA are direct Rip1 proteolytic targets. Our attempts to reconstitute anti-sigma factor processing in *E. coli* by expressing Rip1 and RskA or RsmA were unsuccessful due to constitutive degradation of the mycobacterial anti-sigma factors, even in wild type *E. coli* without Rip1(data not shown).

Phenanthroline induces expression of *rpfC*, a Rip1 dependent gene

ECF sigma factors control gene expression in response to cell envelope stress. In the absence of the activating signal, the ECF regulons are off and therefore genetic ablation of the sigma factor has little or no effect on gene expression. The upstream activating signals for Sigma K, L, and M in *M. tuberculosis* are unknown and target genes have been assigned based on sigma factor over-expression (Agarwal et al., 2006, Raman et al., 2006) or deletion of their cognate anti-sigma factor (Dainese et al., 2006, Said-Salim et al., 2006). Our prior examination of gene expression in the Δ*rip1* strain identified *rpfC* as a strongly under-expressed gene (Makinoshima & Glickman, 2005). In the course of testing for chemical compounds that would activate or inhibit the Rip1 pathway, we identified the metal chelator phenanthroline as an activator of *rpfC* transcription (data not shown) indicating that phenanthroline may be an upstream activator of the Rip1 pathway. This result stimulated a broader examination of phenanthroline induced, Rip1 dependent gene expression.

To examine the full complement of genes controlled through Rip1 in response to phenanthroline, we performed transcriptional profiling using oligonucleotide microarrays representing 4750 ORFs from *M. tuberculosis*. We compared RNA isolated from phenanthroline treated wild type *M. tuberculosis* to phenanthroline treated Δ*rip1* cells. We found relatively few genes were differentially regulated between phenanthroline treated wild type and Δ*rip1* cells (Table S3). Among the regulated genes in these experiments were the iron storage protein *bfrB* and the resuscitation promoting factor *rpfC*, the latter of which was previously identified as differentially regulated in the Rip1 mutant in the absence of phenanthroline (Makinoshima & Glickman, 2005). To interrogate the role of SigK, L, and M in the phenanthroline response, we performed additional microarray experiments comparing RNA isolated from phenanthroline treated wild type *M. tuberculosis* to phenanthroline treated Δ*sigK*, Δ*sigL*, and Δ*sigM* strains (constructed by allelic exchange, see methods and strain table). In contrast to the few differentially regulated genes observed in the Δ*rip1* strain, deficiency of SigK, SigL, or SigM resulted in 14, 31, and 46 genes differentially regulated by phenanthroline compared to wild type cells (Supplementary table S4–S6). We selected four genes for further analysis based either on their regulation in the Rip1 array dataset, or their regulation in multiple sigma factors array datasets (suggesting that these genes might be in the Rip1 pathway). A heat map comparing gene expression of these four genes (*rpfC*, *katG*, *bfrB*, and *kasA*) across all four strains is shown in Figure S2. The pattern of expression of these genes suggests a complex mode of regulation. For example, *katG* is under-expressed in Δ*rip1*, Δ*sigK*, and Δ*sigL*, but not Δ*sigM*, whereas *bfrB* is over-expressed in Δ*rip1* but in none of the sigma factor mutants.

NIH-PA Author Manuscript

NIH-PA Author Manuscript

NIH-PA Author Manuscript

To confirm that the levels of these transcripts (*rpfC*, *katG*, *bfrB*, and *kasA*) were controlled by Rip1 in response to phenanthroline, we performed quantitative RT-PCR for each mRNA in wild type and Δ*rip1* cells with and without phenanthroline treatment. The level of *rpfC* mRNA was 15 fold lower in Δ*rip1* cells compared to wild type (Figure 4A). Phenanthroline induced *rpfC* in wild type cells, but *rpfC* remained under-expressed in phenanthroline treated Δ*rip1* cells (Figure 4A). Similarly, the level of *katG* mRNA was barely detectable in untreated wild type and Δ*rip1* cells (Figure 4B). However, phenanthroline induced *katG* RNA by 9.3 fold in wild type cells, a response that was absent in the Δ*rip1* strain and restored in the *rip1* mutant complemented with wild type *rip1* (Figure 4B). These data indicate that the Rip1 pathway is required to upregulate *katG* expression in response to phenanthroline. Quantitation of *bfrB* mRNA revealed that this gene is overexpressed by 10 fold in Δ*rip1* cells (Figure 4C). Treatment with phenanthroline did not induce *bfrB* in wild type cells, consistent with the repression of ferritins by iron chelation (Rodriguez & Smith, 2003). In contrast, phenanthroline highly induced *bfrB* in Δ*rip1* cells (figure 4C). The Δ*rip1* strain complemented with wild type *rip1* behaved like wild type, demonstrating the *bfrB* dysregulation is due to loss of Rip1(figure 4C). These data indicate that a function of the Rip1 pathway is to suppress *bfrB* transcription. Finally, *kasA* was underexpressed in Δ*rip1* untreated cells compared to wild type, confirming prior microarray data (Makinoshima & Glickman, 2005). However, with phenanthroline treatment *kasA* was repressed in both wild type and Δ*rip1* cells, indicating that phenanthroline induced repression of *kasA* is independent of the Rip1 pathway (Figure 4D). These results identify four genes whose transcriptional regulation is Rip1 dependent and three in which the phenanthroline response requires Rip1 (*rpfC*, *katG* and *bfrB*). Having identified four transcriptional targets of the Rip1 pathway, we sought to test the involvement of Sigma K, L, and M in the regulation of these transcripts.

The role of SigK, SigL, and SigM in control of *katG* expression

Based on our anti-sigma factor cleavage assays, one model of the Rip1 pathway is that Rip1 is required to activate the SigK, SigL, and SigM regulons through cleavage of their transmembrane anti-sigma factors. Without Rip1 proteolysis, these sigma factors will remain tethered to the membrane and therefore be unable to direct RNA polymerase to target promoters. As such, loss of Rip1 may phenocopy some combination of loss of Sigma K, L, M. To explore whether Rip1 dependent phenanthroline responses are a direct consequence of Rip1 proteolysis of one or more anti-sigma factor substrates, we applied the following genetic criteria : 1) phenanthroline-regulated, *rip1*-dependent genes should also be dependent on Sigma K, L or M 2) A given Rip1/sigma factor target should be hyperinduced by deletion of the anti-sigma factor in wild type cells 3) Any phenotype of the Δ*rip1* strain shared with a specific sigma factor mutant should be **reversed** by deletion of the cognate anti-sigma factor (i.e. in a Δ*rip1*Δ (anti-sigma factor) double mutant) because the sigma factor will no longer require Rip1 for activation when the anti-sigma is missing, as has been demonstrated for *E. coli* SigE and *B. subtilis* SigW (Alba et al., 2002, Kanehara et al., 2002, Ellermeier & Losick, 2006).

We first applied the genetic criteria defined above to *katG* using quantitative RT-PCR to measure *katG* mRNA with and without phenanthroline treatment. We observed that phenanthroline induction of *katG* was abolished in Δ*sigK*, and Δ*sigL*, but was unaffected in the Δ*sigM* strain (Figure 4B), suggesting that Rip1 cleavage of anti-SigK and/or anti-SigL activates *katG* transcription. Regulation of *katG* expression in *M. tuberculosis* and other mycobacteria has been extensively investigated. The KatG coding sequence is downstream of the gene encoding FurA, a metal binding transcriptional repressor that responds to oxidative stress (Pym *et al.*, 2001). Transcription of *katG* in *M. tuberculosis* and *M. smegmatis* initiates from two promoters, one upstream of *furA* and one at the 3′ end of the

NIH-PA Author Manuscript

NIH-PA Author Manuscript

NIH-PA Author Manuscript

furA coding sequence (figure 4F;(Master *et al.*, 2001, Milano *et al.*, 2001)). Both p*furA* and p*katG* are induced inside macrophages with different temporal profiles (Master et al., 2001). FurA binds upstream of the *furA* coding sequence and represses transcription of the *furA* promoter by binding an AT rich sequence which overlaps the −35 element (Sala *et al.*, 2003). To determine whether activation of *furA* is also downstream of Rip1/SigK/SigL, we measured *furA* RNA and found that *furA* expression was also Rip1, SigK, and SigL dependent, but SigM independent (figure 4E). The activators of the p*katG* promoter have not been defined, but the 5′ end of the *katG* mRNA is a cytosine residue 17 nucleotides upstream of the last nucleotide of the FurA coding sequence (Milano et al., 2001). Using this transcription start point (TSP) and that of *furA*, we searched for SigK and SigL consensus binding sequences using the experimentally determined TSPs of known SigK targets (*mpt70*, *mpt83*, and *Rv0449* (Rodrigue *et al.*, 2007, Said-Salim et al., 2006)) or SigL targets (*sigL*, *sigB*, *pks10*, *rv2978c*, and *rv1139c* (Dainese et al., 2006, Hahn et al., 2005) using the program MD scan (Liu *et al.*, 2002). This approach identified a SigK −10 and −35 site 5′ of the *katG* TSP but did not identify a SigL site (figure 4F). Although our search included the region 5′ of the *furA* TSP, we did not identify a SigK or SigL site 5′ of *furA*. Coupled with the genetic data presented above, this finding suggests that SigK-RNAP may activate transcription at the *katG* promoter at the 3′ end of *furA*.

Taking into account that phenanthroline can chelate iron and induce oxidative stress, we tested whether the Rip1 dependent activation of *katG* could be reproduced by iron deprivation. We found that *katG* was not induced iron limitation (Figure S3A), consistent with previously published data (Zahrt *et al.*, 2001, Rodriguez *et al.*, 2002). We confirmed that the cells were experiencing iron deprivation by measuring induction of the siderophore biosynthetic gene *mbtB* (Figure S3B). In contrast, we did observe a partial Rip1 dependence of *katG* induction in response to hydrogen peroxide, indicating that phenanthroline may be acting through induction of oxidative stress (Figure S3C).

The role of SigK, SigL, and SigM in Rip1 dependent regulation of *bfrB*, *kasA* and *rpfC*

We next turned our attention to the role of Rip1 in suppressing *bfrB* in response to phenanthroline (figure 4B). Bacterioferritins are iron storage proteins that chelate intracellular iron. These storage molecules also play a major role in defense against oxidative stress because they remove $Fe2^{+}$, which participates in Fenton chemistry with hydrogen peroxide (Arosio *et al.*, 2009). Transcription of bacterioferritins is repressed in low iron and induced in high iron to match iron storage capacity with the availability of excess iron (Gold *et al.*, 2001). As such, iron chelation by phenanthroline should repress *bfrB* expression, a response that is defective when the Rip1 pathway is inactivated (Figure 4C). We measured *bfrB* mRNA and found that over-expression of *bfrB* in untreated cells was not present in any sigma factor mutant (Figure 4C) and that phenanthroline did not induce *bfrB* in any of the Sigma KLM mutants (Figure 4C). These data indicate that *bfrB* overexpression is a *rip1* dependent phenotype, but that loss of any one sigma factor in the Rip1 pathway does not reproduce this phenotype. The most likely explanation for these findings is that *bfrB* overexpression in the Rip1 null is due to simultaneous inactivation of 2 or 3 sigma factor regulons. An alternative explanation is that *bfrB* overexpression is independent of the anti-sigma factor substrates identified here.

To determine whether *rpfC* and *kasA* are directly regulated by Rip1 cleavage of anti-SigKLM, we measured *rpfC* and *kasA* mRNAs in the Δ*sigK*, Δ*sigL*, and Δ*sigM* strains. We confirmed that *rpfC* is under-expressed in the Δ*rip1* strain, but this phenotype was not shared by any of the Sigma factor mutants (figure 4A), indicating that Rip1 dependent activation of *rpfC* is independent of any one of the three Rip1 cleaved anti-Sigma factors identified here. Similar results were obtained for *kasA*. Specifically, *kasA* RNA was 2.8 fold less abundant in Δ*rip1* cells than wild type cells. However, the suppression of *kasA* RNA by

NIH-PA Author Manuscript

NIH-PA Author Manuscript

NIH-PA Author Manuscript

phenanthroline present in wild type cells was still observed in Δ*rip1* cells (figure 4D). None of the individual sigma factor mutants phenocopied the degree of *kasA* under-expression of the *rip1* mutant, although *kasA* was mildly under-expressed in the SigK and SigL mutants. In summary, we find that three Rip1 regulated genes (*rpfC*, *kasA*, and *bfrB*) are regulated independently of any single sigma factor. In contrast, *katG* expression requires two sigma factors and Rip1 for activation.

Phenanthroline induction of *katG* requires Rip1 cleavage of RskA and RslA

The participation of SigK and SigL in *katG* expression afforded an opportunity to test whether Rip1 cleavage of RskA or RslA activated *katG*. In order to further dissect the molecular mechanism of *katG* induction upon phenanthroline treatment, we monitored the levels of this transcript in various Rip1 pathway double mutants in the presence or absence of phenanthroline. Deletion of anti-SigK, anti-SigL, or anti-SigM caused over-expression of *katG* in untreated cells by approximately 2–3 fold (Figure 5A). Strikingly, phenanthroline induced *katG* expression was restored in the Δ*rip1* strain by deletion of *rskA* (Δ*rip1*Δ*rskA*), indicating that *rip1* is only required to induce *katG* when *rskA* is present (Figure 5A). In contrast, phenanthroline induced *katG* expression was partially restored in the Δ*rip1*/Δ*rslA* strain to a level similar to the derepressed basal level in theΔ*rslA* strain, indicating that *katG* is expressed, but not induced by phenanthroline in this strain. This data demonstrates that the lack of *katG* induction in the Δ*rip1* strain is due to failed cleavage of RskA. The failure of phenanthroline induction of *katG* in theΔ*rip1*/Δ*rslA* strain is presumably caused by the presence of RskA and its requirement for Rip1 for cleavage.

Phenanthroline does not induce site-one cleavage of Rip1 pathway anti-sigma factors

The data presented above indicates that phenanthroline induces *katG* and that this response requires SigK and SigL activation by Rip1 cleavage of RskA and RslA. We considered two possible mechanisms for this observation. It is possible that phenanthroline is acting as an upstream activator of the Rip1 pathway by initiating site one cleavage of RskA/RslA. Alternatively, it is possible that phenanthroline is acting intracellularly to relieve repression by metal dependent repressors (such as FurA), thereby exposing a Rip1/SigK/SigL dependent positive signal that activates *katG* transcription. To distinguish these two possibilities, we tested whether phenanthroline treatment induced anti-Sigma factor site one cleavage, which can be assayed by the accumulation of C terminally truncated intermediates of RskA and RslA in Δ*rip1* cells (see figure 2). In wild type cells, treatment with phenanthroline did not affect the abundance of full length RskA or RslA (Figure 5B). In *rip1* mutant cells, treatment with phenanthroline also did not result in accumulation of C terminally truncated RslA (Figure 5B, lane 6 vs. lane 8). C terminally truncated RskA actually disappeared with phenanthroline treatment (Figure 5B, lane 2 vs. lane 4). These data suggest that phenanthroline does not directly activate the site one cleavage of the anti-sigma factors, but rather serves as a chemical tool that unmasks the previously cryptic contribution of positive regulators (Rip1, SigK, SigL) to *katG* transcription, possibly through the relief of FurA mediated repression.

Candidate gene approach to identify S1P(s) of RskA, RslA, and RsmA

Having identified three transmembrane anti-sigma factors as Rip1 substrates and shown that these substrates undergo processing by site one protease(s), we sought to identify S1Ps using a candidate gene approach, To identify potential S1Ps of the Rip1 pathway, we took advantage of our cleavage assay using N-terminal Hemagglutinin tagged anti-Sigma factors. Loss of Rip1 results in accumulation of truncated forms of anti-SigK, L, and M (Figure 2), suggesting that loss of the protease that initiates Site-1 cleavage should prevent the steady-state accumulation of the truncated proteins in the *rip1* mutants. This type of analysis was

NIH-PA Author Manuscript

NIH-PA Author Manuscript

NIH-PA Author Manuscript

used to identify PrsW as the protease responsible for the Site-1 cleavage of RsiW in *Bacillus subtilis* (Ellermeier & Losick, 2006,Heinrich & Wiegert, 2006).

We implemented a reverse genetic approach in order to identify potential S1Ps of the Rip1 pathway. We used MEROPS (http://merops.sanger.ac.uk/), a protein database that uses hierarchical and structure based classification of peptidases in order to identify likely S1Ps annotated in the *M. tuberculosis* genome. We tested Rv3668c, PepA, and Rv1043c, all of which are orthologs of DegS, the S1P of the SigE proteolytic cascade of *Escherichia coli* (Ades, 2008), by deleting the genes encoding these proteases in both wild type and Δ*rip1 M. tuberculosis*. In the *rv3668c*, *pepA*, and *rv1043c* mutants, RskA, Rsla, and RsmA were detected at their predicated unprocessed molecular sizes as expected (Figure S4 A-C). Loss of *Rv3668c* (Figure S4A), *pepA* (Figure S4B), or Rv1043c(Figure S4C) in the Δ*rip1* background did not affect the accumulation of truncated products of RskA, RslA, and RsmA. Taken together, we believe that these results indicate that these three S1P candidates are not individually required for the processing of the three anti-sigma factors of the Rip1 pathway. Further exploration of the S1Ps for the Rip1 pathway will require additional candidate gene approaches or genetic screening.

Discussion

RIP of multiple substrates

We have shown that a single RIP protease has three distinct anti-Sigma factor substrates, RskA, RslA, and RsmA. This is a novel feature of the Rip1 pathway of *M. tuberculosis* because other bacterial S2Ps have single anti-Sigma factor substrates, although some S2Ps do have multiple substrates in mammalian cells (Ye *et al.*, 2000, Zhang *et al.*, 2006) and in *B. subtilis* (Schobel et al., 2004, Bramkamp *et al.*, 2006). Our present model of the Rip1 pathway is presented in Figure 6. Rip1/SigK/SigL activate *katG* transcription in response to phenanthroline. KatG activation occurs through Rip1 cleavage of anti-SigK and anti-SigL. Additionally, the Rip1 pathway suppresses *bfrB* transcription in untreated cells and in response to phenanthroline, implicating Rip1 in regulation of iron metabolism. However, loss of Sigma K, L, or M does not cause overexpression of *bfrB*. Similarly, Rip1 positively regulates expression of *kasA* and *rpfC*, but this phenotype is not present in the individual sigma factor mutants. Taken together, these results suggest either that combinatorial loss of Sigma K, L, or M is responsible for the *bfrB*, *kasA*, and *rpfC* regulation in the Δ*rip1* strain, or that Rip1 has additional substrates not yet identified that control *bfrB, kasA, and rpfC*.

Phenanthroline and the Rip1 pathway

We have used phenanthroline in this initial dissection of signal transduction through the Rip1 pathway. Phenanthroline stress of *M. tuberculosis* has revealed a clear role for the Rip1 pathway is regulating two genes involved in defense against oxidative stress, *katG and bfrB*. Our data strongly suggest that phenanthroline does not result in increased cleavage of RskA/RslA, but likely relieves FurA repression, which reveals regulation of *katG* by SigK/SigL through basal cleavage of RskA/RslA by Rip1. Further studies will be required to determine whether SigK and/or SigL containing RNAP directly transcribes the *katG* gene, either acting at pFurA or pKatG. Published data about the existence of a promoter at the 3′ end of FurA (pKatG) are conflicting. In one study, the 3′ end of *M. tuberculosis* FurA can directed expression of a GFP reporter in vitro and in macrophages and was inducible by hydrogen peroxide (Master et al., 2001). In another study, a promoter at the 3′ end of FurA was active in *M. smegmatis*, although this promoter was not induced by hydrogen peroxide (Milano et al., 2001). A later study suggested that the appearance of the shorter *katG* mRNA was due to transcript cleavage rather than transcriptional initiation (Sala *et al.*, 2008). The basis for suggesting transcript cleavage was the lack of a demonstrable promoter at the 3′ end of FurA

NIH-PA Author Manuscript

NIH-PA Author Manuscript

NIH-PA Author Manuscript

when assayed in *M. smegmatis*. However, *M. smegmatis* does not contain a SigK ortholog and therefore these studies may not reflect the regulation that occurs in *M. tuberculosis*, especially in light of our identification of a SigK recognition site at pKatG.

Although the regulation of KatG expression has been extensively investigated at the promoter level, less is known about the signal transduction systems that regulate its expression in response to extracytoplasmic stress. The data presented here demonstrates that transmembrane signal transduction through the Rip1 pathway is an important regulatory system for *katG* expression, and suggests that the virulence defect in the Δ*rip1* strain may in part be due to KatG dysregulation (Ng *et al.*, 2004). Although phenanthroline is a useful chemical tool for some *rip1* dependent genes, the true in vivo activators of the Rip1 system remain to be identified. Based on our results, we hypothesize that they are likely to include a combination of stresses (possibly sensed through a multiplicity of S1Ps to be determined) such as iron deprivation and oxidative stress. Monitoring the expression of *M. tuberculosis* target genes identified in this study during the course of infection may provide us with clues about the nature of these signals. Ultimately, identification of the S1P(s) responsible for the cleavage of anti-SigK,L, and M is paramount in order to further understand the molecular mechanism responsible for Rip1 dependent gene expression and virulence attenuation.

Our initial description of Rip1 of *M. tuberculosis* established a major virulence role for this pathway. The data presented here suggests that this severe in vivo phenotype may be due to the simultaneous inactivation of three Sigma factor pathways. This model is consistent with the previously reported mild *in vivo* phenotypes for individual sigma factor mutants, including *sigM* (Karls *et al.*, 2006, Agarwal et al., 2006) and *sigL* (Hahn et al., 2005, Dainese et al., 2006) which do not phenocopy the severe attenuation of the Δ*rip1* strain. The virulence phenotype of an *M. tuberculosis sigK* null mutant has not been reported. Cleavage of three anti-sigma factor substrates by Rip1 may allow *M. tuberculosis* to integrate multiple extracellular stresses encountered during growth in the host, and respond to these stresses with an appropriate and robust transcriptional response. This model can now be addressed genetically by testing double and triple sigma factor mutants (ΔKM, ΔKL, ΔLM, ΔKLM) in virulence assays.

Experimental Procedures

Bacterial Strains and Growth Conditions

All strains for this study are listed in Supplementary Table 2 (Table S2). *M. tuberculosis* strains (Erdman) were grown at 37°C in 7H9 (broth) or 7H10 (agar) (Difco) media with OADC enrichment, 0.5% glycerol, 0.05% Tween 80 (broth). *M. smegmatis* strains were cultured at 37°C on LB or Middlebrook 7H9 medium (Difco) containing 0.5% dextrose, 0.5% glycerol and 0.05% Tween 80. When appropriate, Hygromycin B (Boehringer Mannheim) at 50 μg/ml, Kanamycin (Sigma) at 20 μg/ml or 1,10-phenanthroline (Sigma) at 1 mM was added into medium. For iron-depleted growth conditions, the strains were cultivated in pH6.6 glycerol alanine salts including 0.05% Tween80 (GAST) medium with or without iron as described previously (De Voss et al., 2000, Manabe *et al.*, 2005).

Plasmid construction expressing HA-tagged anti-sigma factors

We constructed N-terminally HA-tagged RsdA (Rv3413c), RsmA (Rv3912), RskA (Rv0444c) and RslA (Rv0736) by amplifying the open reading frame with oHMG253_254, oHMG255_256, oHMG251_268 and oHMG269_270, respectively. All HA tagged anti-Sigma factors are expressed from the GroEL promoter on episomal plasmids using the vector PMV261kan. To make the C-terminal truncated version of anti-sigma factors, we used the same upstream primers for full length anti-sigmas (see above) and downstream

NIH-PA Author Manuscript

NIH-PA Author Manuscript

NIH-PA Author Manuscript

primers named oHMG333 for RsdA192, oHMG334 for RsmA154, oHMG335 for RskA160 and oHMG336 for RslA161.

Mutant Construction and Removal of Hygromycin Cassette

All Rip1 pathway mutants were constructed via specialized transduction using the temperature sensitive phage phAE87 (Bardarov *et al.*, 1997, Barkan *et al.*, 2009). To remove the *hyg*^{r} cassette from *rip1* mutants, MGM309 cells were transformed with pMSG381-1, a plasmid expressing HSP60-Cre, which contains an unstable MF1 origin of replication. After 3 weeks of growth on 7H10 plates containing kanamycin, transformants were picked and grown in 7H9 media without antibiotics for 1 week. After reaching confluence, 10μl of these cultures were subcultured into 10ml of fresh 7H9 media without antibiotics. After 1 week of growth, cells from these cultures were struck onto nonselective 7H10 agar plates. Single colonies from these plates were scored for kanamycin and hygromycin sensitivity. Loss of *hyg*^{r} through LoxP recombination was verified using PCR.

Quantitative RT-PCR

mRNA levels for *katG*, *bfrB*, *kasA*, *rpfC*, and *mbtB* were measured with quantitative RT-PCR. For all phenanthroline experiments, 1 mM of phenanthroline solution (in methanol) was added to a culture at OD600 ~0.5. 30 min after induction, the cells were pelleted, and resuspended in Trizol reagent (Invitrogen). For control treatment, an equal volume of methanol was used. For hydrogen peroxide treatment, 10mM of H_2O_2 was added to a culture at OD600 ~0.5. for 1 hour, the cells were pelleted, and resuspended in Trizol reagent. Cells were disrupted mechanically with Zirconia beads in a FastPrep instrument (QBiogene). After extraction with chloroform, RNA was precipitated with isopropyl alcohol and washed with 75% ethanol and dried. The RNA was treated with RNase free DNase I for use with RNeasy Columns (QIAGEN). About 1 μg of DNase I treated RNA was reverse-transcribed using Superscript III reverse transcriptase (Invitrogen) and random primers (Invitrogen). Real-time RT-PCR was performed using SYBR Green and an Opticon2 real time fluorescence detector (MJ Research). Single amplification products for each PCR reaction were confirmed by melting curve analysis. All experiments are the mean of biologic triplicates. The primers used in real RT-PCR are listed in Table S1. The cycle threshold value (Ct) obtained for each gene of interest (GOI) was normalized with that of *sigA*, a housekeeping gene, in the same RNA sample by the formula $\Delta Ct = Ct_{GOI} - Ct_{SigA}$. Relative levels of individual genes were calculated using the following formula: $2^{-(\Delta Ct)}$ to generate an expression level for each gene of interest.

DNA Microarrays

RNA was prepared from 20 ml of *M. tuberculosis* cultures as described above and subsequently treated with QIAGEN's RNAeasy RNA clean-up protocol. cDNA libraries were made using the Stratagene Fairplay kit. cDNA coupled to fluorescent dyes Cy3 and Cy5 (GE Healthcare) were hybridized to gene chips spotted four times with oligos representing 4750 *M. tuberculosis* ORFs (obtained from through the Pathogen Functional Genomics Resource Center). All experiments were performed in triplicate and analyzed using Partek Genomics Suite software using intensity dependent Lowess normalization. Significance was determined with a *p*-value confidence level set to ≤5%. Significant fold changes were assigned to $\log_2$ values higher or lower than 0.5.

Western blot analysis

Briefly,10mL cultures were grown to an OD600 ~0.5, pelleted, and washed twice with NP-40 lysis buffer (9.32mM Na2PO4, 0.68mM NaH2PO4, 150mM NaCl, 0.25% NP-40) supplemented with complete protease Inhibitor cocktail (Roche). The final cell pellet was

NIH-PA Author Manuscript

NIH-PA Author Manuscript

NIH-PA Author Manuscript

resuspended in 100μL of buffer. Cells were disrupted mechanically with Zirconia beads in a FastPrep instrument (QBiogene) for a total of 3× with a 5-min incubation on ice between disruptions. After an additional incubation on ice for 10 min, 100μL of 2× SDS loading buffer was added to each lysate. Samples were boiled for 10 min and equal volumes were loaded onto NuPAGE 4-12% Bis Tris polyacrylamide gels (Invitrogen). After electrophoresis, gels were transferred to a nitrocellulose membrane and probed with mouse monoclonal anti-HA antibody (Covance). Anti-Dlat antibodies were used as a loading control. HRP conjugated anti-mouse antibody (Zymed) was used as a secondary probe. ECL (GE Healthcare) and XAR film (Kodak, Rochester, NY) were used to visualize the protein bands.

Supplementary Material

Refer to Web version on PubMed Central for supplementary material.

Acknowledgments

We thank Feng Gao for outstanding technical support and Carl Nathan and Ruslana Bryk for providing the anti-Dlat antibody. We are grateful to members of the Glickman laboratory and Tom Silhavy for their helpful discussions. This work was supported by NIH grant AI083041 to JGS, AI080628 and AI53417 to MSG and The Burroughs Wellcome Fund Investigators in the Pathogenesis of Infectious Diseases award (MSG). HM was supported as a Fellow for Research Abroad Japan Society for the Promotion of Science (JSPS). The microarrays used in this study were obtained through NIAID's Pathogen Functional Genomics Resource Center, managed and funded by Division of Microbiology and Infectious Diseases, NIAID, NIH, DHHS and operated by the J. Craig Venter Institute

References

Ades SE. Regulation by destruction: design of the sigmaE envelope stress response. Curr Opin Microbiol. 2008; 11:535–540. [PubMed: 18983936]

Agarwal N, Woolwine SC, Tyagi S, Bishai WR. Characterization of the Mycobacterium tuberculosis sigma factor SigM: virulence assessment and identification of SigM-dependent genes. Infect Immun. 2006

Alba BM, Leeds JA, Onufryk C, Lu CZ, Gross CA. DegS and YaeL participate sequentially in the cleavage of RseA to activate the sigma(E)-dependent extracytoplasmic stress response. Genes Dev. 2002; 16:2156–2168. [PubMed: 12183369]

Arosio P, Ingrassia R, Cavadini P. Ferritins: a family of molecules for iron storage, antioxidation and more. Biochim Biophys Acta. 2009; 1790:589–599. [PubMed: 18929623]

Bardarov S, Kriakov J, Carriere C, Yu S, Vaamonde C, McAdam RA, Bloom BR, Hatfull GF, Jacobs WR Jr. Conditionally replicating mycobacteriophages: a system for transposon delivery to Mycobacterium tuberculosis. Proc Natl Acad Sci U S A. 1997; 94:10961–10966. [PubMed: 9380742]

Barkan D, Liu Z, Sacchettini JC, Glickman MS. Mycolic acid cyclopropanation is essential for viability, drug resistance, and cell wall integrity of Mycobacterium tuberculosis. Chem Biol. 2009; 16:499–509. [PubMed: 19477414]

Bramkamp M, Weston L, Daniel RA, Errington J. Regulated intramembrane proteolysis of FtsL protein and the control of cell division in Bacillus subtilis. Mol Microbiol. 2006; 62:580–591. [PubMed: 17020588]

Campbell EA, Greenwell R, Anthony JR, Wang S, Lim L, Das K, Sofia HJ, Donohue TJ, Darst SA. A conserved structural module regulates transcriptional responses to diverse stress signals in bacteria. Mol Cell. 2007; 27:793–805. [PubMed: 17803943]

Council BMR. A controlled trial of 2-month, 3-month, and 12-month regimens of chemotherapy for sputum-smear-negative pulmonary tuberculosis. Results at 60 months. Am Rev Respir Dis. 1984; 130:23–28. [PubMed: 6377997]

NIH-PA Author Manuscript

NIH-PA Author Manuscript

NIH-PA Author Manuscript

Dainese E, Rodrigue S, Delogu G, Provvedi R, Laflamme L, Brzezinski R, Fadda G, Smith I, Gaudreau L, Palu G, Manganelli R. Posttranslational regulation of Mycobacterium tuberculosis extracytoplasmic-function sigma factor sigma L and roles in virulence and in global regulation of gene expression. Infect Immun. 2006; 74:2457–2461. [PubMed: 16552079]

De Voss JJ, Rutter K, Schroeder BG, Su H, Zhu Y, Barry CE 3rd. The salicylate-derived mycobactin siderophores of Mycobacterium tuberculosis are essential for growth in macrophages. Proc Natl Acad Sci U S A. 2000; 97:1252–1257. [PubMed: 10655517]

Dye C. Global epidemiology of tuberculosis. Lancet. 2006; 367:938–940. [PubMed: 16546542]

Dye C, Espinal MA, Watt CJ, Mbiaga C, Williams BG. Worldwide incidence of multidrug-resistant tuberculosis. J Infect Dis. 2002; 185:1197–1202. [PubMed: 11930334]

Ellermeier CD, Losick R. Evidence for a novel protease governing regulated intramembrane proteolysis and resistance to antimicrobial peptides in Bacillus subtilis. Genes Dev. 2006; 20:1911–1922. [PubMed: 16816000]

Gold B, Rodriguez GM, Marras SA, Pentecost M, Smith I. The Mycobacterium tuberculosis IdeR is a dual functional regulator that controls transcription of genes involved in iron acquisition, iron storage and survival in macrophages. Mol Microbiol. 2001; 42:851–865. [PubMed: 11722747]

Hahn MY, Raman S, Anaya M, Husson RN. The Mycobacterium tuberculosis extracytoplasmic-function sigma factor SigL regulates polyketide synthases and secreted or membrane proteins and is required for virulence. J Bacteriol. 2005; 187:7062–7071. [PubMed: 16199577]

Heinrich J, Hein K, Wiegert T. Two proteolytic modules are involved in regulated intramembrane proteolysis of Bacillus subtilis RsiW. Mol Microbiol. 2009; 74:1412–1426. [PubMed: 19889088]

Heinrich J, Wiegert T. YpdC determines site-1 degradation in regulated intramembrane proteolysis of the RsiW anti-sigma factor of Bacillus subtilis. Mol Microbiol. 2006; 62:566–579. [PubMed: 17020587]

Kanehara K, Ito K, Akiyama Y. YaeL (EcfE) activates the sigma(E) pathway of stress response through a site-2 cleavage of anti-sigma(E), RseA. Genes Dev. 2002; 16:2147–2155. [PubMed: 12183368]

Karls RK, Guarner J, McMurray DN, Birkness KA, Quinn FD. Examination of Mycobacterium tuberculosis sigma factor mutants using low-dose aerosol infection of guinea pigs suggests a role for SigC in pathogenesis. Microbiology. 2006; 152:1591–1600. [PubMed: 16735723]

Kinch LN, Ginalski K, Grishin NV. Site-2 protease regulated intramembrane proteolysis: sequence homologs suggest an ancient signaling cascade. Protein Sci. 2006; 15:84–93. [PubMed: 16322567]

Liu XS, Brutlag DL, Liu JS. An algorithm for finding protein-DNA binding sites with applications to chromatin-immunoprecipitation microarray experiments. Nat Biotechnol. 2002; 20:835–839. [PubMed: 12101404]

Makinoshima H, Glickman MS. Regulation of Mycobacterium tuberculosis cell envelope composition and virulence by intramembrane proteolysis. Nature. 2005; 436:406–409. [PubMed: 16034419]

Makinoshima H, Glickman MS. Site-2 proteases in prokaryotes: regulated intramembrane proteolysis expands to microbial pathogenesis. Microbes and infection / Institut Pasteur. 2006; 8:1882–1888. [PubMed: 16731018]

Manabe YC, Hatem CL, Kesavan AK, Durack J, Murphy JR. Both Corynebacterium diphtheriae DtxR(E175K) and Mycobacterium tuberculosis IdeR(D177K) are dominant positive repressors of IdeR-regulated genes in M. tuberculosis. Infect Immun. 2005; 73:5988–5994. [PubMed: 16113319]

Master S, Zahrt TC, Song J, Deretic V. Mapping of Mycobacterium tuberculosis katG promoters and their differential expression in infected macrophages. J Bacteriol. 2001; 183:4033–4039. [PubMed: 11395468]

Milano A, Forti F, Sala C, Riccardi G, Ghisotti D. Transcriptional regulation of furA and katG upon oxidative stress in Mycobacterium smegmatis. J Bacteriol. 2001; 183:6801–6806. [PubMed: 11698368]

Ng VH, Cox JS, Sousa AO, MacMicking JD, McKinney JD. Role of KatG catalase-peroxidase in mycobacterial pathogenesis: countering the phagocyte oxidative burst. Mol Microbiol. 2004; 52:1291–1302. [PubMed: 15165233]

NIH-PA Author Manuscript

NIH-PA Author Manuscript

NIH-PA Author Manuscript

Pym AS, Domenech P, Honore N, Song J, Deretic V, Cole ST. Regulation of catalase-peroxidase (KatG) expression, isoniazid sensitivity and virulence by furA of Mycobacterium tuberculosis. Mol Microbiol. 2001; 40:879–889. [PubMed: 11401695]

Raman S, Puyang X, Cheng TY, Young DC, Moody DB, Husson RN. Mycobacterium tuberculosis SigM positively regulates Esx secreted protein and non-ribosomal peptide synthesis genes and down regulates virulence-associated surface lipid synthesis. J Bacteriol. 2006

Rodrigue S, Brodeur J, Jacques PE, Gervais AL, Brzezinski R, Gaudreau L. Identification of mycobacterial sigma factor binding sites by chromatin immunoprecipitation assays. J Bacteriol. 2007; 189:1505–1513. [PubMed: 17158685]

Rodriguez GM, Smith I. Mechanisms of iron regulation in mycobacteria: role in physiology and virulence. Mol Microbiol. 2003; 47:1485–1494. [PubMed: 12622807]

Rodriguez GM, Voskuil MI, Gold B, Schoolnik GK, Smith I. ideR, An essential gene in mycobacterium tuberculosis: role of IdeR in iron-dependent gene expression, iron metabolism, and oxidative stress response. Infect Immun. 2002; 70:3371–3381. [PubMed: 12065475]

Said-Salim B, Mostowy S, Kristof AS, Behr MA. Mutations in Mycobacterium tuberculosis Rv0444c, the gene encoding anti-SigK, explain high level expression of MPB70 and MPB83 in Mycobacterium bovis. Mol Microbiol. 2006

Sala C, Forti F, Di Florio E, Canneva F, Milano A, Riccardi G, Ghisotti D. Mycobacterium tuberculosis FurA autoregulates its own expression. J Bacteriol. 2003; 185:5357–5362. [PubMed: 12949087]

Sala C, Forti F, Magnoni F, Ghisotti D. The katG mRNA of Mycobacterium tuberculosis and Mycobacterium smegmatis is processed at its 5′ end and is stabilized by both a polypurine sequence and translation initiation. BMC Mol Biol. 2008; 9:33. [PubMed: 18394163]

Schnappinger D, Ehrt S, Voskuil MI, Liu Y, Mangan JA, Monahan IM, Dolganov G, Efron B, Butcher PD, Nathan C, Schoolnik GK. Transcriptional Adaptation of Mycobacterium tuberculosis within Macrophages: Insights into the Phagosomal Environment. J Exp Med. 2003; 198:693–704. [PubMed: 12953091]

Schobel S, Zellmeier S, Schumann W, Wiegert T. The Bacillus subtilis sigmaW anti-sigma factor RsiW is degraded by intramembrane proteolysis through YluC. Mol Microbiol. 2004; 52:1091–1105. [PubMed: 15130127]

Stallings CL, Stephanou NC, Chu L, Hochschild A, Nickels BE, Glickman MS. CarD is an essential regulator of rRNA transcription required for Mycobacterium tuberculosis persistence. Cell. 2009; 138:146–159. [PubMed: 19596241]

Urban S. Making the cut: central roles of intramembrane proteolysis in pathogenic microorganisms. Nat Rev Microbiol. 2009; 7:411–423. [PubMed: 19421188]

Ye J, Rawson RB, Komuro R, Chen X, Dave UP, Prywes R, Brown MS, Goldstein JL. ER stress induces cleavage of membrane-bound ATF6 by the same proteases that process SREBPs. Mol Cell. 2000; 6:1355–1364. [PubMed: 11163209]

Zahrt TC, Song J, Siple J, Deretic V. Mycobacterial FurA is a negative regulator of catalase-peroxidase gene katG. Mol Microbiol. 2001; 39:1174–1185. [PubMed: 11251835]

Zhang K, Shen X, Wu J, Sakaki K, Saunders T, Rutkowski DT, Back SH, Kaufman RJ. Endoplasmic reticulum stress activates cleavage of CREBH to induce a systemic inflammatory response. Cell. 2006; 124:587–599. [PubMed: 16469704]

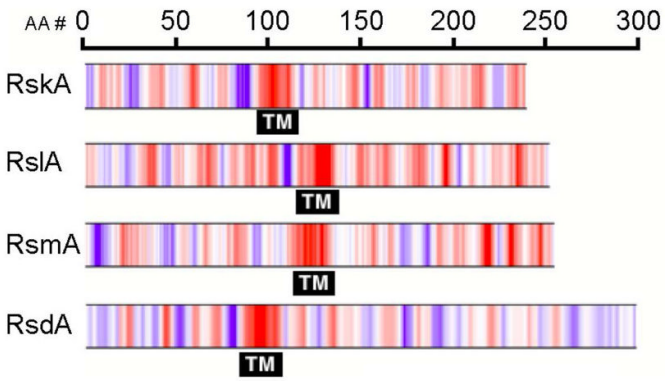

Figure 1. Four *M. tuberculosis* anti-sigma factors are predicted transmembrane proteins

The indicated proteins are pictured schematically with amino acid hydrophobicity as a color scale from blue (hydrophilic) to red (hydrophobic) according to the Kyte-Doolittle scale, with white being neutral. The predicted transmembrane domains (TM) are indicated and amino acid numbers are indicated at the top.

NIH-PA Author Manuscript
NIH-PA Author Manuscript
NIH-PA Author Manuscript

NIH-PA Author Manuscript
NIH-PA Author Manuscript
NIH-PA Author Manuscript

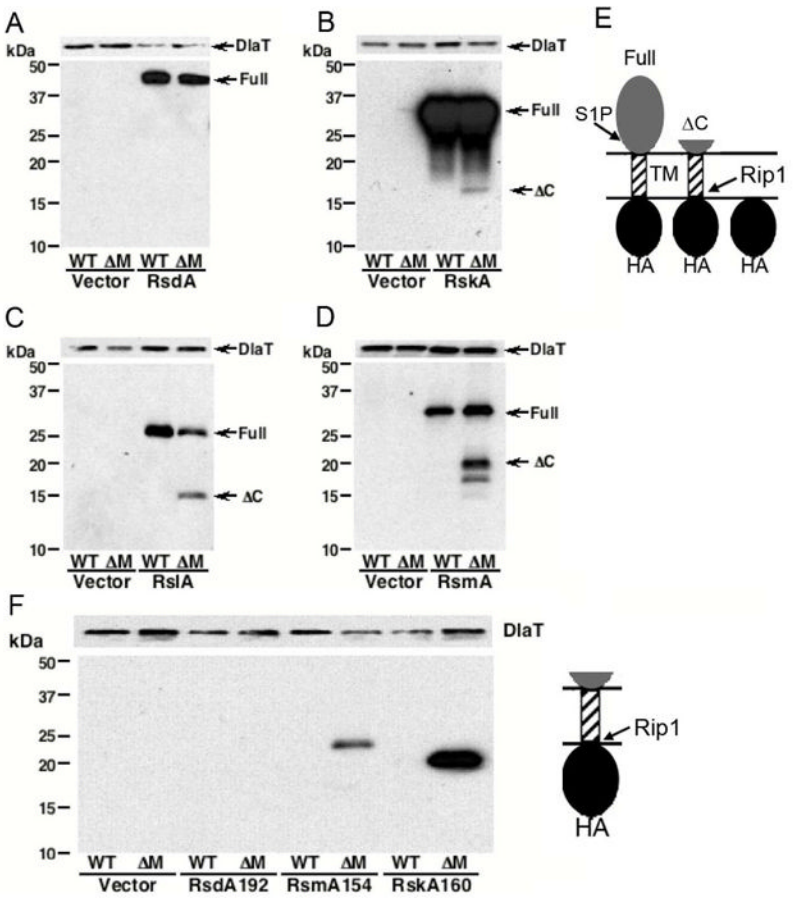

Figure 2. Rip1 is required for proteolytic processing of three anti-Sigma factors

Four anti-sigma factors RsdA (A), RskA (B), RslA (C), and RsmA (D) with N-terminal Hemagglutinin epitope tags were expressed in wild type *M. tuberculosis* (WT lanes), or the *rip1* null mutant (ΔM lanes). HA tagged proteins were detected by immunoblotting using anti-HA antibodies in parallel with the loading control anti-DLAT. Panel E is a schematic representation of predicted cleavage products after the action of Site one (S1P) and site two proteases (S2P).

F. Rip1 constitutively degrades truncated RsmA and RskA, but not RsdA. C terminally truncated anti-Sigma factors with N terminal Hemagglutinin tags were expressed in wild type (WT) or *rip1* mutant (ΔM) *M. tuberculosis*. Protein lysates were probed with either anti-HA or the loading control anti-DLAT.

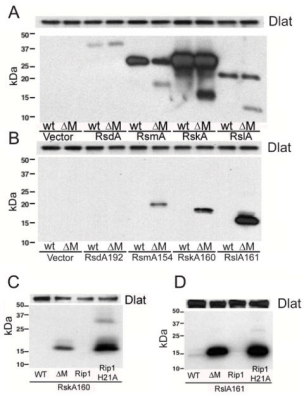

Figure 3. Molecular requirements for Rip1 anti-sigma factor cleavage reconstituted in *M. smegmatis*

A. HA tagged anti-sigma factors used in Figure 2A-D were expressed either in wild type *M. smegmatis* (WT), or the ΔMSmeg*rip1* strain (M). Proteins were detected either with anti-HA or anti-DLAT (loading control).

B. C terminally truncated, HA tagged, anti-sigma factors accumulate in the absence of MSmeg*rip1*

C terminally truncated anti-sigma factors were expressed in wild type *M. smegmatis* or the MSmeg*rip1* null mutant and monitored by anti HA western blotting.

C-D. Rip1 proteolytic activity is required for anti sigma factor processing. The MSmeg*rip1* null mutant bearing RskA160 (C) or RslA161 (D) was complemented with *M. tuberculosis* Rip1 or Rip1-H21A.

NIH-PA Author Manuscript NIH-PA Author Manuscript NIH-PA Author Manuscript

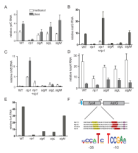

Figure 4. Role of Sigma K, Sigma L, and Sigma M in Rip1 dependent gene expression

A. Quantitative RT-PCR of *rpfC* RNA in Wild type (WT), Δ*rip1*, Δ*sigK*, Δ*sigL*, *and* Δ*sigM* either treated with methanol (solvent control, white bar), or treated with 1mM phenanthroline for 30 minutes (grey bar). Y axis shows the level of *katG* transcript normalized to RNA encoding the housekeeping sigma factor SigA. Plotted values are means of biologic triplicates and error bars are standard deviation.

B. Quantitative RT-PCR of *katG* RNA in Wild type (WT), Δ*rip1*, genetically complemented (Δ*rip1+rip1*), Δ*sigK*, Δ*sigL*, *and* Δ*sigM* either treated with methanol (white bar), or treated with 1mM phenanthroline for 30 minutes (grey bar). Y axis shows the level of *katG* transcript normalized to RNA encoding the housekeeping sigma factor SigA. Plotted values are means of biologic triplicates and error bars are standard deviation.

C. Quantitative RT-PCR of *bfrB* RNA in Wild type (WT), Δ*rip1*, Δ*rip1+rip1*, Δ*sigK*, Δ*sigL*, *and* Δ*sigM* either treated with methanol control (white bar), or treated with 1mM phenanthroline for 30 minutes (grey bar). Y axis shows the level of *bfrB* transcript normalized to RNA encoding the housekeeping sigma factor SigA. Plotted values are means of biologic triplicates and error bars are standard deviation.

D. Quantitative RT-PCR of *kasA* RNA in phenanthroline treated cells with the same legend presented in A.

E. Quantitative RT-PCR of *furA* RNA in phenanthroline treated cells with the same legend presented in A.

F. SigK consensus at the 5′ proximal promoter of *katG*. The consensus was derived using computational analysis of known SigK target promoters (*mpt70*, *mpt83*, and *rv0499*) and the entire *furA-katG* genetic locus. Purple letters represent experimentally derived transcriptional start sites (see text), the FurA binding site is colored blue, −10 elements are colored red, and −35 elements are colored yellow.

NIH-PA Author Manuscript NIH-PA Author Manuscript NIH-PA Author Manuscript

NIH-PA Author Manuscript

NIH-PA Author Manuscript

NIH-PA Author Manuscript

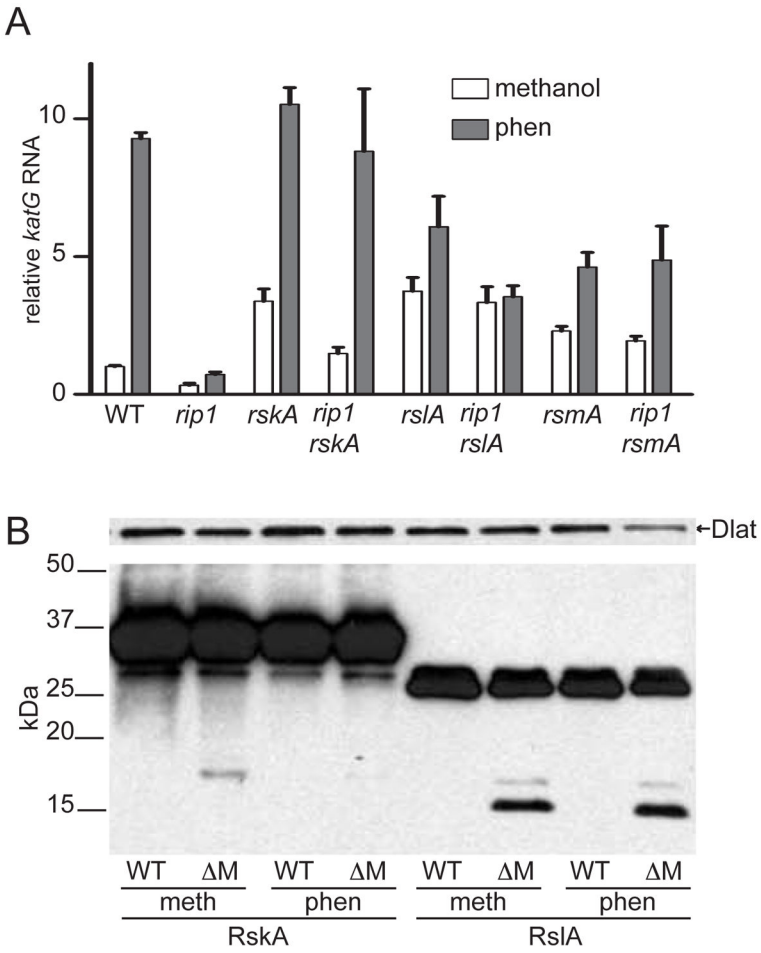

Figure 5. Phenanthroline induction of *katG* requires Rip1 cleavage of RskA and RslA

A. Quantitative RT-PCR of *katG* RNA in various Rip1 pathway mutants either treated with methanol control (white bar), or treated with 1mM phenanthroline for 30 minutes (grey bar). Y axis shows the level of *katG* transcript normalized to RNA encoding the housekeeping sigma factor SigA. Plotted values are means of biologic triplicates and error bars are standard deviation.

B. Western blot analysis of HA tagged anti-sigma factors (RskA/RslA) expressed in wild type *M. tuberculosis* (WT lanes), or the *rip1* null mutant (ΔM lanes). Cells were grown in the presence of methanol (meth) and 1mM phenanthroline (phen) for 30min prior to analysis. Protein lysates were probed with either anti-HA or the loading control anti-DLAT.

NIH-PA Author Manuscript
NIH-PA Author Manuscript
NIH-PA Author Manuscript

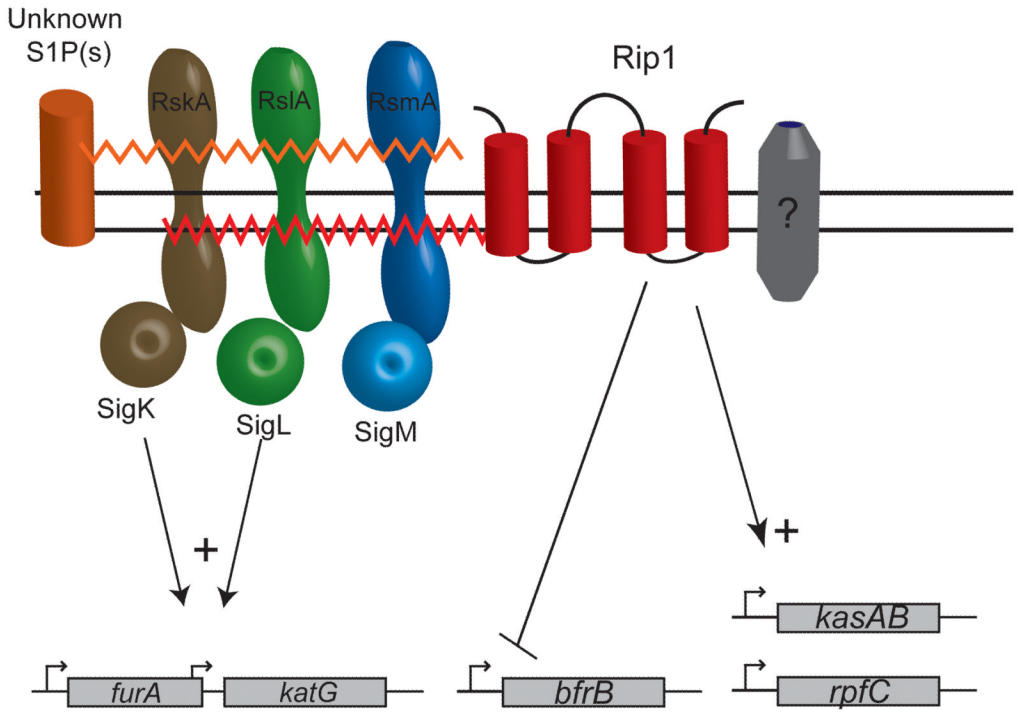

Figure 6. Present model of the Rip1 pathway

The orange and red lines represent cleavage of three anti-Sigma factors, RskA, RslA, and RsmA, by unknown S1P(s) and Rip1 respectively. Rip1 cleavage of RskA and RslA releases SigK and SigL respectively, which activates transcription of *katG*. In addition, our data identifies Rip1 dependent regulation of *kasA*, *bfrB*, and *rpfC* which is independent of Sigma K, L, or M. A functional copy of Rip1 is required to repress *bfrB* transcription and activate *kasAB* and *rpfC* transcription. We have represented these regulatory interactions directly from Rip1, although we envision that they arise either through some combination of Sigma KLM, or through as yet unidentified additional substrates of Rip1 (pictured as the grey cylinder).